PREDICTIONS OF THE TEMPERATURE PROFILE WITHIN COMPOSITE SHEETS DURING PRE-HEATING

J. E. Cunningham* and P. F. Monaghan+

This paper deals with advances made to a mathematical model which simulates the pre-heating of fiber and fabric reinforced thermoplastic composite laminates prior to press forming. The model predicts the transient temperature distribution within the laminates throughout the pre-heating process for various heating techniques. In this paper, attention is focused on two particular developments that improve on the previous model. A modelling technique that incorporates models of both quartz and ceramic heaters into the overall infra-red heating simulation is dealt with first. Secondly, the procedure used to model the transfer process from the heating rig to the forming press is described. Software predictions are then compared to experimental data to verify the model accuracy.

NOMENCLATURE

A	area, m^2	t	time, secs.
C_p	specific heat capacity, J $kg^{-1}K^{-1}$	Nu	Nusselt number, dimensionless
F	view factor, dimensionless	Re	Reynolds number dimensionless
h	convection coefficient W $m^{-2}K^{-1}$	Pr	Prandtl number, dimensionless
N	number of enclosure surfaces	Ra	Rayleigh number, dimensionless
q	heat flow, W	Gr	Grashof number, dimensionless
k	thermal conductivity W $m^{-1}K^{-1}$	Fo	Fourier number, dimensionless
T	temperature, K	Bi	Biot number, dimensionless

Greek

ε	emissivity, dimensionless
ρ	density, kg m^3
	reflectivity, dimensionless
σ	Stefan Boltzmann constant
τ	Transmissivity, dimensionless
α	thermal diffusivity, m^2 s^{-1}

Subscripts

k	surface k
s	surface s
o	outgoing heat flow
i	incoming heat flow
rad	radiation
conv	convection
surr	surroundings
eff	effective
∞	surrounding air temp.

* Thermal Engineering Research Unit, Manufacturing Research Centre, University College Galway, Ireland.

+ Q-SET Ltd, Campus Technology Park, Upper Newcastle, Galway, Ireland.

INTRODUCTION

Recent interest in the aircraft and automotive industries has focused on incorporating composite materials into commercial aircraft and automobile designs. Materials such as fiber or fabric reinforced thermoplastics offer huge weight savings over conventional isotropic materials such as steel or aluminium. Press forming of structural shapes from these materials has become popular because of the high processing speeds involved[1].

Previously, a trial and error approach to the press forming of parts was the norm. This approach did not provide a fundamental understanding of the process and this lack of understanding has contributed to the high cost of composite components and composites in general[2]. However, with the recent interest in press forming, efforts have been directed at developing a better understanding of the process with a view to optimizing it.

Much of the focus of research in the press forming area has been on the forming and cooling stages, with very little research being done on the pre-heating process. The pre-heating stage, however, is very important as incorrect pre-heating can cause problems such as delamination and surface burning.

There are various forms of pre-heating with infra-red heating, contact heating and convection heating being the most common[3]. Each form of heating has its advantages and disadvantages; Infra-red heating is fast and flexible but it can produce non-uniform temperature distributions[4]; Contact heating is the most efficient but there are problems with matrix adhesion to the platens[3]; Convection heating provides a very uniform temperature distribution but is very slow[3]. The choice of technique is influenced by a variety of factors such as part size, cost of equipment, speed of heating and material forming temperature.

An important stage in the pre-heating process is the transfer process from the heating rig to the forming press. Usually, pre-heating and forming are carried out separately at different locations. Therefore, it is necessary to move the heated laminate in order to form it, a process that can result in substantial heat loss depending on the method and environment of transfer. If the heat loss during transfer is a significant factor, it is often necessary to 'overheat' the laminate to ensure that it is hot enough to form when it reaches the press. Methods of transfer vary from complex tray and rail systems to simple hand transfer.

The long term objective of a joint project recently completed by the authors was to provide software tools to predict and improve the thermoforming of fiber and fabric reinforced thermoplastic sheet materials for structural applications[1]. The task of the authors within the project was to provide a software tool that would predict the transient temperature distribution within composite laminates from the start of heating to the point when the forming press made first contact with the heated laminate. Various heating techniques were to be modelled. This software tool is described in detail in Cunningham *et al*[5]. This paper focuses on recent refinements to the model described in that paper and, specifically, it describes two major improvements:

- The heat-up of both quartz and ceramic infra-red heaters is now modelled, with only a heater type and heater power required as input
- The transfer process from the heating rig to the forming press is modelled

REVIEW

Turner and Ash developed models to predict the radiant heat flux produced by single and multiple quartz heaters on a planar surface, with and without reflectors[6,7]. These analyses were based on a classical method which uses the following assumptions: (1) No interaction between the filament and quartz is modelled, the surface of the quartz tube is considered the sole source of radiation, (2) The radiant energy is assumed to be uniformly distributed over the lamp(s) surface, (3) The emitted radiation from the quartz is diffuse, (4) The fraction of irradiation absorbed, transmitted and reflected by a surface is diffuse and gray (independent of wavelength) and (5) Radiation reflected back to the source is lost. Turner and Ash[8] modelled the radiant flux distribution produced by quartz heaters using advanced analytical and statistical methods. Their model analyses the interaction between the filament(s), quartz tube(s), reflector(s) and the surroundings. Each of these models predicts a steady state heat flux and no attempt is made to model transient effects.

Radiant heat transfer to flat and inclined composite panels using quartz heaters has been modelled by Cassidy[9,10] and Sweeney *et al*[11] has investigated the different parameters involved in the infra-red heating process using quartz heaters. The authors have also investigated heat transfer to composite panels using various heating techniques[5]. Each of these models is again based on a classical analysis with associated assumptions similar to those used by Turner and Ash[6,7]. Because of these assumptions these models all require experimentally measured heater temperatures and an 'effective' emissivity value for the heaters. The resultant heat fluxes calculated are used as inputs to finite difference models to predict the temperature distribution within the composite. Brogan *et al*[12] removes the need for heater temperatures and 'effective' emissivities by modelling the interaction between the filament and the quartz tubes using a net radiation method[13]. However, he assumes uniform heat flux to the composite and he treats the heater banks as one combined heater, thus not allowing for zonal power distributions.

The work described in this paper advances on the above models in the following way:

- A model of the heat-up of individual quartz heaters is built into the models of the pre-heating of composite panels using infra-red heating described in Cunningham *et al*[5]
- A similar model of the heat-up of individual ceramic heaters is also built into the Cunningham *et al*[5] model
- A model to predict the heat loss during the transfer process from the heating rig to the forming press has been developed

OVERALL MODEL DESCRIPTION

A general description of the overall model is given here. For a more detailed description of this model refer to Cunningham *et al*[13].

There are six analysis options in the software. Three of the options are for Infra-red heating and there is one option each for contact heating, convection heating and a technique specific to a project partner[14] that will be referred to as platen radiant heating for the rest of this paper. Each analysis option is separate and distinct but they all apply similar solution techniques. Firstly, the geometry and test conditions are inputted. Based on these inputs the transient temperature distribution within the laminate being heated is calculated in two steps:

- The heat flux to the laminate is calculated (or from it during transfer)
- The new temperature distribution within the laminate is calculated

These steps are then repeated over time giving the transient temperature profile.

The heat flux to the laminate during heating may involve certain combinations of conduction, convection or radiation heat transfer depending on the heating technique. In general, where radiation heat transfer occurs, classical enclosure analysis techniques[9,15] are used to predict heat fluxes. However, for Infra-red heating, a more complex net radiation method[13] can also be used to predict heat fluxes. This analysis is described in detail later. Convection heat fluxes are predicted using convection heat transfer coefficients that are estimated with empirical correlations[15]. Conduction heat fluxes are predicted with contact resistance values taken from the literature[15,16]. The method of determining heat fluxes during transfer is described in detail later.

The temperature distribution within the laminate is predicted using finite difference techniques. Depending on the heating technique and analysis, 1-D, 2-D or 3-D temperature distributions are predicted. Anisotropic conduction is modelled in the 2-D and 3-D cases. It should be noted that in any of the heating techniques where walls are present the transient wall temperature is also modelled.

NET RADIATION METHOD[13]

The following assumptions apply to the net radiation method:

- All surfaces are isothermal, diffuse and gray
- A uniform temperature can be assigned to the entire volume of the transparent surfaces

For an enclosure as shown in Fig. 1 with N surfaces, m of which are opaque, the overall energy balance for the opaque surfaces can be written as:

$$q_k = q_{o,k} - q_{i,k} \qquad (1 \le k \le m) \qquad (1)$$

The outgoing energy, $q_{o,k}$, consists of emitted and reflected energy as follows:

$$q_{o,k} = \varepsilon_k \sigma T_k^4 + (1 - \varepsilon_k) q_{i,k} \qquad (1 \le k \le m) \qquad (2)$$

For the *N-m* transparent surfaces, the overall energy balance can be written as:

$$q_k = q_{o,k} - q_{i,k} + q_{l,k} - q_{e,k} \qquad (1+m \le k \le N) \qquad (3)$$

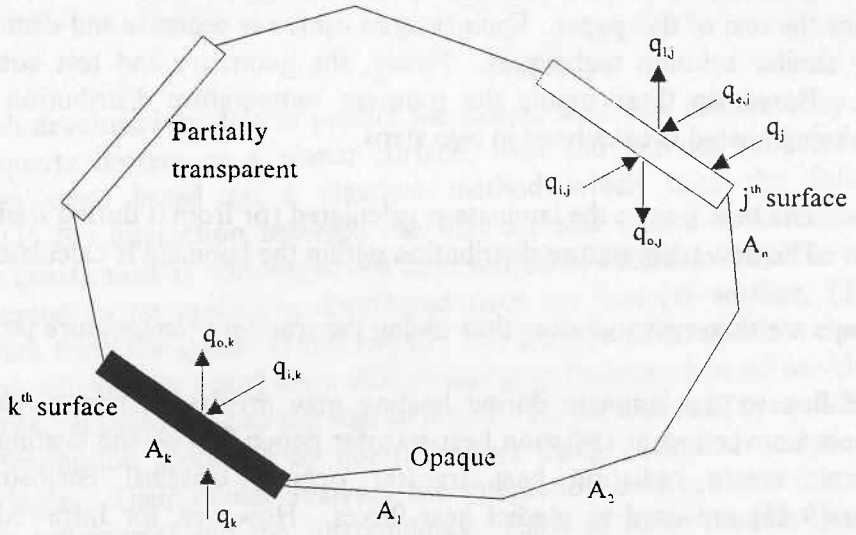

Fig. 1 General enclosure for enclosure analysis, consisting of opaque and partially transparent walls

where $q_{l,k}$ is the outgoing energy from the outer surface of the transparent window and $q_{e,k}$ is the incident energy on the outer surface of the transparent window. The outgoing energy from the inner surface consists of emitted, reflected and transmitted energy as follows:

$$q_{o,k} = \varepsilon_k \sigma T_k^4 + \rho_k q_{i,k} + \tau_k q_{e,k} \qquad (m+1 \le k \le N) \qquad (4)$$

The heat flux lost from the outer surface of the transparent window, $q_{l,k}$, is given by:

$$q_{l,k} = \varepsilon_k \sigma T_k^4 + \rho_k q_{e,k} + \tau_k q_{i,k} \qquad (m+1 \le k \le N) \qquad (5)$$

The incident radiant energy can be related to the outgoing energy for the N surfaces in the enclosure using view factor relationships[17], giving:

$$q_{i,k} = \sum_{j=1}^{N} q_{o,j} F_{kj} \qquad (1 \le k \le N) \qquad (6)$$

APPLICATION OF THE NET RADIATION METHOD TO A QUARTZ HEATING SYSTEM

The quartz heating setup can be divided into the following types of surfaces (See Fig. 2)

- Walls or hypothetical surfaces
- Composite (2 sides)

- Top or bottom surface if one sided heating
- Quartz outer surface -- oven side
- Quartz inner surface -- oven side
- Quartz inner surface -- case side
- Quartz outer surface -- case side
- Case

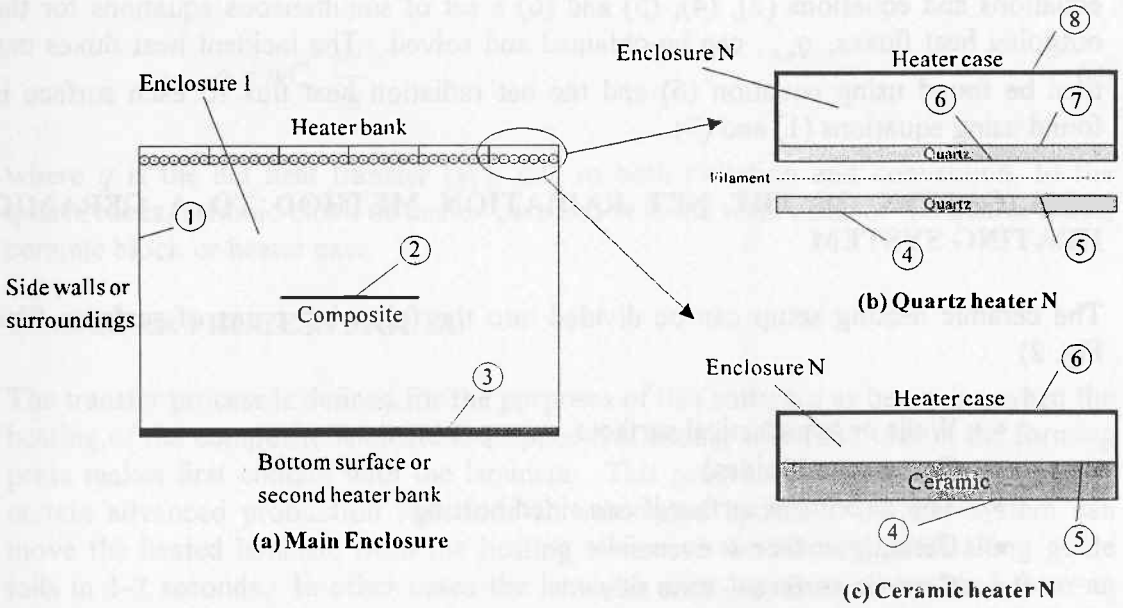

Fig. 2 Diagram of a) main enclosure and surfaces for IR heating, b) Heater enclosure and surfaces for Quartz heaters and c) Heater enclosure and surfaces for Ceramic heaters

When the net radiation method described above is applied to the quartz heating system shown in Fig. 2 the following added assumptions are made:

1) All surfaces except the quartz surfaces are opaque
2) The quartz tubes can be treated as two parallel flat transparent windows having the same dimensions as the heater
3) The steel reflective cases act as one surface
4) The outgoing radiation from the steel case is only incident on the quartz outer surface on the case side
5) Any radiation from the large enclosure is only incident on the quartz outer surface on the oven side
6) The radiant energy from the filament incident on the surface of the windows is uniform
7) There is no heat transfer between adjacent heaters

Assumptions 1, 2, 4, 5 and 7 above imply that the system can be reduced to a series of $N+1$ enclosures where N is the number of heaters in the system. The N represents the enclosures between the heater case (S_8) and the quartz outer surface on the case side(S_7) while the *1* represents the enclosure formed by the quartz outer surface on the oven side(S_4) and the rest of the oven(S_1, S_2, S_3) (See Fig. 2). The analysis of the N enclosures is linked to the analysis of the main enclosure by the relationship between the energy incident on the quartz inner surfaces (S_5, S_6). This is given by:

$$q_{i,5} = q_{o,6} + q_{e,5} \tag{7}$$

$$q_{i,6} = q_{o,5} + q_{e,6} \tag{8}$$

where $q_{e,5}$ and $q_{e,6}$ are the incident radiant heat fluxes from the filament. Using these equations and equations (2), (4), (5) and (6) a set of simultaneous equations for the outgoing heat fluxes, $q_{o,k}$, can be obtained and solved. The incident heat fluxes can then be found using equation (6) and the net radiation heat flux to each surface is found using equations (1) and (3).

APPLICATION OF THE NET RADIATION METHOD TO A CERAMIC HEATING SYSTEM

The ceramic heating setup can be divided into the following types of surfaces (See Fig. 2)

- Walls or hypothetical surfaces
- Composite (2 sides)
- Top or bottom surface if one sided heating
- Ceramic surface -- oven side
- Ceramic surface -- case side
- Case

When the net radiation method is applied to the ceramic heating system shown in Fig. 3 the following added assumptions are made:

1) All surfaces are opaque
2) The ceramic can be treated as two parallel flat surfaces having the same dimensions as the heater
3) The steel reflective cases act as one surface
4) There is no heat transfer between adjacent heaters

Assumptions 1, 2 and 4 above again imply that the system can be reduced to a series of $N+1$ enclosures where N is the number of heaters in the system. The N represents the enclosures between the heater case (S_6) and the ceramic surface on the case side(S_5) while the 1 represents the enclosure formed by the ceramic surface on the oven side(S_4) and the rest of the oven(S_1, S_2, S_3) (See Fig. 2). The analysis of the N enclosures is linked to the analysis of the main enclosure by the ceramic itself which has a surface in each enclosure (Surfaces S_4 and S_5).

Using equations (2) and (6) a set of simultaneous equations for the outgoing heat fluxes, $q_{o,k}$, can be obtained and solved. The incident heat fluxes can then be found using equation (6) and the net radiation heat flux to each surface is found using equation (1).

UPDATING HEATER COMPONENT TEMPERATURES

The above radiation analysis, along with the natural convection and conduction analyses, are carried out at each timestep during the transient analysis. The temperatures of the quartz tubes, if quartz heaters are used, ceramic blocks, if ceramic heaters are used, and the heater case are all updated after each timestep using a lumped capacitance approach. This is based on the following energy balance:

$$q = mC_p \frac{dT}{dt} \tag{9}$$

where q is the net heat transfer [W], due to both radiation and convection, to the quartz tubes, ceramic block or heater case and m is the total mass of the quartz tubes, ceramic block or heater case.

TRANSFER PROCESS MODEL

The transfer process is defined for the purposes of this software as beginning when the heating of the composite laminate is stopped and ending when the tool in the forming press makes first contact with the laminate. This process can take many forms. In certain advanced production situations an automated hydraulic transfer system can move the heated laminate from the heating station to the forming press along guide rails in 1-2 seconds. In other cases the laminate must be removed by hand from an oven, carried across a room to a press, placed in position for forming and then the press is activated. Such a process could take up to 1 minute. Therefore, it is difficult to develop a general model for a process that can vary so much. However, by making some general assumptions, the modelling task can be simplified. These assumptions are:

- All effects of the support system for the laminate are neglected
- Heat given off during laminate crystallization is negligible
- A clear and definite boundary exists between conditions inside and outside the heating system
- When exiting the heating system, the part of the laminate still in the system neither gains nor loses heat
- The effects of any vertical motion the laminate undergoes are neglected
- The effects caused by air being pushed in front of the closing press are neglected

Based on these assumptions the transfer process can be split into three stages (See Fig. 3):

- Laminate exiting pre-heating station
- Laminate moving between pre-heating station and forming press
- Laminate sitting in forming press while tool descends

Each of these stages involves heat loss to the surroundings by radiation and convection. The modelling approach to these heat loss processes is described in the

next section. During stage 1 of the transfer process, the laminate is partly inside and partly out of the heating station and is moving with a certain velocity. The model recognizes how much of the laminate is actually out at any particular timestep. The section still inside is assumed to neither gain nor lose heat while the section that is out loses heat to the surroundings by radiation and convection. This heat loss can occur from the front, sides, top and bottom of the laminate. During stage 2, all of the laminate is now outside and the back of the laminate can also lose heat to the surroundings. During stage 3, the laminate is motionless in the forming press and natural convection heat transfer dominates, with all surfaces losing heat.

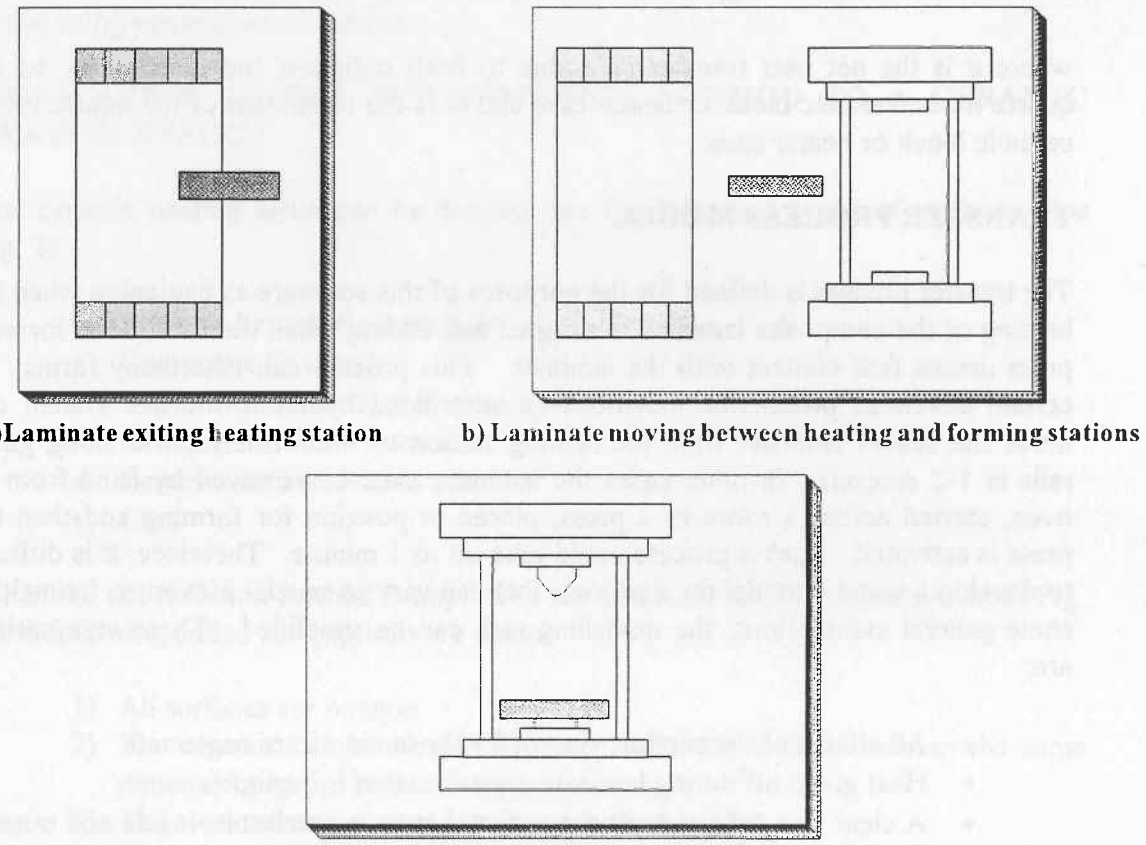

a)Laminate exiting heating station **b) Laminate moving between heating and forming stations**

c) Laminate sitting in press while punch descends

Fig. 3 Diagram of stages of transfer a) Laminate exiting heating rig, b) Laminate moving between heating and forming rig and c) Laminate in position in forming press

Heat Loss Modelling

Radiation losses

Radiation losses are assumed to depend only on the temperatures of the surface location and the surroundings and are given by the following equation:

$$q_{rad} = \varepsilon\sigma A_s (T_s^4 - T_{surr}^4) \tag{10}$$

where A_s is the area of the surface in question, T_s is the temperature of the surface in question and T_{surr} is the temperature of the surroundings. This equation can be linearized for use in finite difference calculations in the following manner:

$$q_{rad} = h_{rad} A_s (T_s - T_{surr}) \tag{11}$$

where h_{rad} , the radiation heat transfer coefficient, is given by:

$$h_{rad} = \varepsilon\sigma(T_s + T_{surr})(T_s^2 + T_{surr}^2) \tag{12}$$

Convection losses

The convection heat losses are given by:

$$q_{conv} = h_{conv} A_s (T_s - T_{surr}) \tag{13}$$

where h_{conv} , the convection heat transfer coefficient, is calculated from the following relation for the Nusselt number, Nu_x:

$$Nu_x = \frac{h_x x}{k} \tag{14}$$

and x is the characteristic length of the laminate and is assumed to be the distance from the leading edge of the laminate to the node in question in all cases, unless otherwise stated.

The convection losses can be either forced convection, natural convection or both and the Nusselt number varies depending on which type of loss occurs and also on which part of the laminate convection heat transfer is occurring from.

Convection from top and bottom surfaces

For the top and bottom surfaces the model first checks if the Reynolds number, Re_x, is greater than 5.0E+05. If it is then turbulent conditions exist, if not, the flow is laminar.

For laminar conditions, combined forced and natural convection is assumed and the following equation, taken from Churchill[18], is used to calculate the Nusselt number:

$$(Nu - Nu_o)^{7/2} = \left[A_F \, \mathrm{Re}^{1/2} \, \mathrm{Pr}^{1/3} \, f_F(\mathrm{Pr})\right]^{7/2} \pm \left[A_N (Ra . f_N(\mathrm{Pr}))^{1/3}\right]^{7/2} \tag{15}$$

The value of A_F is 0.339 for local values with a uniform surface temperature and the value of A_N is 0.456 for similar circumstances. Nu_0 is a fudge factor to improve the accuracy of the equation with the empirical results obtained and has a value of 0.5. The positive sign in the equation applies to the top surface of the laminate and the minus sign applies to the bottom surface. The terms $f_F(Pr)$ and $f_N(Pr)$ are given by :

$$f_F(\mathrm{Pr}) = \left[1 + \left(\frac{C_F}{\mathrm{Pr}}\right)^{2/3}\right]^{-1/4} \tag{16a}$$

$$f_N(\mathrm{Pr}) = \left[1 + \left(\frac{C_N}{\mathrm{Pr}}\right)^{9/16}\right]^{-16/9} \tag{16b}$$

where C_N has a value of 0.312.

For turbulent conditions, natural convection is neglected and the Nusselt number is given by the following correlation for forced convection[15] :

$$Nu_x = 0.0296\,\mathrm{Re}^{4/5}\,\mathrm{Pr}^{1/3} \tag{17}$$

Convection from the side surfaces

For convection from the side surfaces the model first checks whether forced, natural or mixed convection conditions occur. This is done using the following relation[15] to determine which form of convection takes place:

$$\frac{Gr_L}{\mathrm{Re}_L^2} >> 1 \Rightarrow \text{Natural}; \qquad \frac{Gr_L}{\mathrm{Re}_L^2} << 1 \Rightarrow \text{Forced}; \qquad \frac{Gr_L}{\mathrm{Re}_L^2} \approx 1 \Rightarrow \text{Mixed} \tag{18}$$

If forced convection occurs then the model checks the Reynolds number to see if laminar or turbulent conditions exist. If the flow is laminar then the Nusselt number is given by[15]:

$$Nu_x = 0.332\,\mathrm{Re}^{1/2}\,\mathrm{Pr}^{1/3} \tag{19}$$

If the flow is turbulent then the Nusselt number is given by equation (17).

If natural convection occurs then the flow is considered laminar and the Nusselt number is given by:

$$Nu_x = -\left(\frac{Gr_x}{4}\right)^{1/4} g(\mathrm{Pr}) \tag{20}$$

where the characteristic length, x, is the distance from the bottom edge of the vertical surface and the function $g(Pr)$ is correlated to within 5% by an interpolation formula of the form[19]:

$$g(\mathrm{Pr}) = \frac{0.75\,\mathrm{Pr}^{1/2}}{(0.609 + 1.221\,\mathrm{Pr}^{1/2} + 1.238\,\mathrm{Pr})^{1/4}} \tag{21}$$

If mixed convection occurs, then the free and forced convection Nusselt numbers are calculated separately using equations (17) or (19) and (20) and then added together. They must be calculated separately due to their different characteristic lengths.

Convection from the front and back surfaces

For the front and back surfaces the convection coefficients are assumed to be equal to the convection coefficients for the corresponding nodes on the top front and back edges respectively.

Updating laminate temperature

The radiation and convection heat losses are calculated at each timestep using the techniques described above. They are then used as boundary conditions for a form of analysis procedure used to predict the transient temperature profile within the

composite laminate. This analysis procedure breaks the laminate into a series of 2-D layers as shown in Fig. 4. The bottom layer is analyzed first, followed by the next layer up, and so on until the top layer has been analyzed and the new temperature profile calculated. 2-D finite difference equations can be developed and solved for each layer. However, the temperature of each node depends on the temperature of the nodes directly above and below it as well as adjacent in-plane nodes. The temperature of the node below the node in question is known because the layers are solved in series, starting with the bottom one. The temperature of the node above the node in question is estimated using an analytical solution for a three dimensional structure that is described below. These two temperatures are then included as boundary conditions to the 2-D finite difference equations for each layer which are solved at each timestep to give the 3-D transient temperature distribution in the laminate. The advantage of this method of solution over a full 3-D analysis is that it requires less computer memory as less data is stored during each timestep.

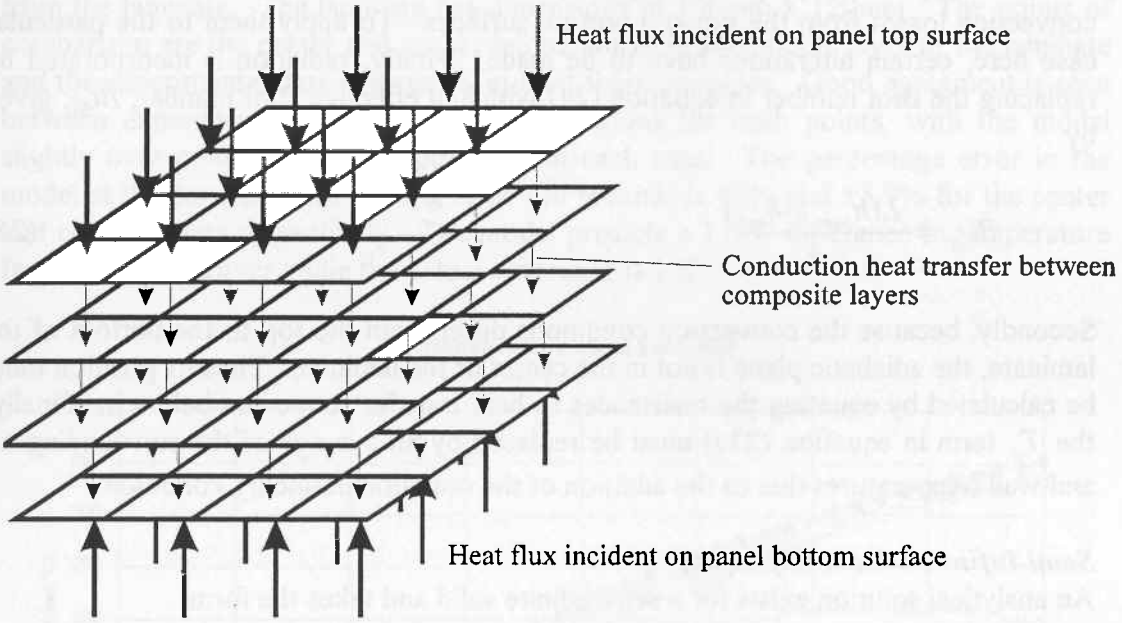

Fig. 4 Modelling of composite laminate as a series of 2-D layers

Analytical solution

The analytical solution used is a combination of three analyses using two analytical solution techniques. These are[15]:

- A Plane Wall Analysis applied through the thickness of the laminate
- A Semi-infinite Solid Analysis applied across the width of the laminate
- A Semi-infinite Solid Analysis applied along the length of the laminate

Plane wall analysis[20]

An analytical solution for a plane wall exists and is of the form:

$$\theta^* = \sum_{n=1}^{\infty} C_n . \exp(-\xi_n^2 Fo) Cos(\xi_n x^*) \qquad (22)$$

where x^* is the dimensionless distance of the node in question from the adiabatic plane and θ^* and C_n are given by equations (23a) and (23b) respectively with T_i being the initial temperature of the node in question.

$$\theta^* = \frac{T - T_\infty}{T_i - T_\infty} \qquad (23a); \qquad C_n = \frac{4Sin\xi_n}{2\xi_n + Sin(2\xi_n)} \qquad (23b)$$

The discrete values (eigenvalues) of ξ_n are positive roots of the transcendental equation shown in equation (24) and the first four roots of this equation approximate the solution and are tabulated in [15]:

$$\xi_n \tan \xi_n = Bi \qquad (24)$$

The above equations apply to a simplified case with no radiation heat losses and equal convection losses from the top and bottom surfaces. To apply them to the particular case here, certain alterations have to be made. Firstly, radiation is incorporated by replacing the Biot number in equation (24) with and effective Biot number, Bi_{eff}, given by:

$$Bi_{eff} = \frac{L(h_{conv} + h_{rad})}{k} \qquad (25)$$

Secondly, because the convection conditions differ from the top to the bottom of the laminate, the adiabatic plane is not in the center of the laminate. Thus its position must be calculated by equating the resistances to heat transfer above and below it. Finally, the T_∞ term in equation (23a) must be replaced by an average of the surrounding air and wall temperatures due to the addition of the radiation boundary condition.

Semi-infinite solid analysis[20]

An analytical solution exists for a semi-infinite solid and takes the form:

$$\frac{T(x,t) - T_i}{T_\infty - T_i} = erfc\left(\frac{x}{2\sqrt{\alpha t}}\right) - \left[\exp\left(\frac{hx}{k} + \frac{h^2 \alpha t}{k^2}\right)\right]\left[erfc\left(\frac{x}{2\sqrt{\alpha t}} + \frac{h\sqrt{\alpha t}}{k}\right)\right] \qquad (26)$$

where the expression *erfc(w)* is the *complementary error function* and is given by the formula:

$$erfc(w) = 1 - erf(w) \qquad (27)$$

and the expression *erf(w)* is the *Gaussian error function* and is tabulated in [15].

Once again, certain modifications have to be made to apply this solution to the laminate heating model. The h value in equation (26) must be replaced by an effective heat transfer coefficient to allow for the radiation heat transfer. Also, the T_∞ term must be modified as for the plane wall case.

The exact analytical solution is achieved by combining the above solutions for the three analyses used as shown below:

$$\frac{T(x,t)-T_\infty}{T_i-T_\infty} = \left.\frac{T(x,t)-T_\infty}{T_i-T_\infty}\right|_{\substack{Plane\\Wall}} \cdot \left.\frac{T(x,t)-T_\infty}{T_i-T_\infty}\right|_{\substack{Length\\Semi-infinite\\Solid}} \cdot \left.\frac{T(x,t)-T_\infty}{T_i-T_\infty}\right|_{\substack{Width\\Semi-infinite\\Solid}} \quad (28)$$

RESULTS

Infra-red Heater Models

Quartz heating

Fig. 5 shows model predictions compared to experimental data for an 8 ply uni-directional APC2/AS4 laminate heated from both sides in an enclosed oven using quartz heaters. The heaters are all set to a power of 600W and they are 300mm away from the laminate. The laminate has dimensions of 120mm x 120mm. The points of comparison are the center and corner temperatures of the middle layer of the laminate and the experimental data is given by in-built thermocouples. Good agreement is seen between experimental data and model predictions for both points, with the model slightly over-predicting the temperatures in each case. The percentage error in the model at the conclusion of heating after 400 seconds is +6% and +5.9% for the center and corner points respectively. The model predicts a 1.6°C difference in temperature from center to corner while the actual difference is 1°C.

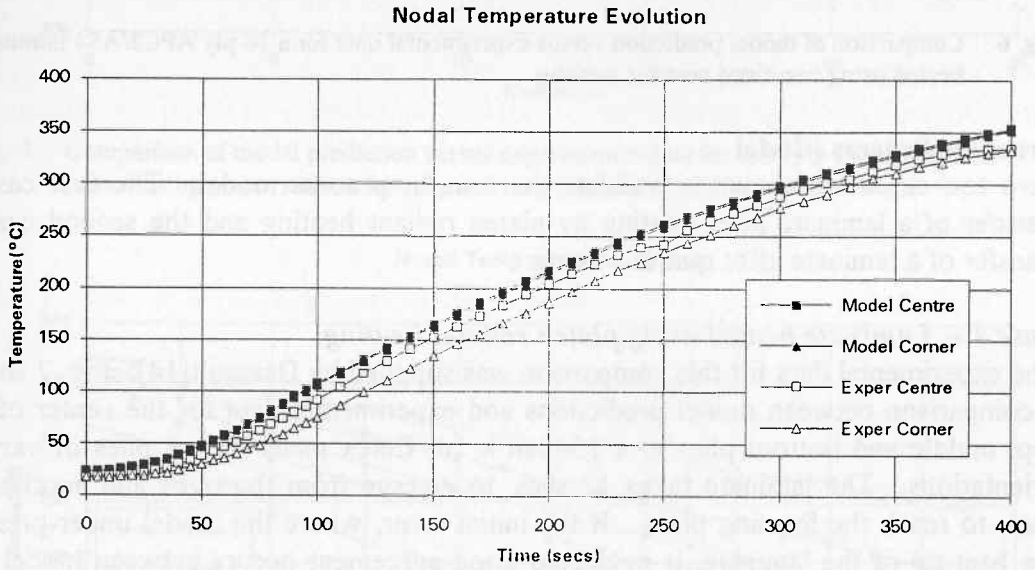

Fig. 5 Comparison of model prediction versus experimental data for an 8 ply APC2/AS4 laminate heated using two sided quartz heating

Ceramic heating

Fig. 6 shows a model prediction compared to experimental data for a 16 ply uni-directional APC2/AS4 laminate heated from both sides in an open oven using ceramic heaters. The heaters are arranged in three zones, an outer ring, a central ring and an interior zone, and they are 100mm away from the laminate. The laminate has dimensions of 130mm x 150mm. The points of comparison are the center temperatures of the top, middle and bottom layers of the laminate and the experimental

data is given by in-built thermocouples. For both the model and experimental data, the heat-up curves for the three nodes are almost coincident so for clarity only the bottom nodal data is shown. Good agreement is seen between experimental data and model prediction with the model slightly under-predicting the temperature. The percentage error in the model at the conclusion of heating after 130 seconds is -0.5%. The model predicts a 1°C difference in temperature from center to surface which corresponds to the actual difference.

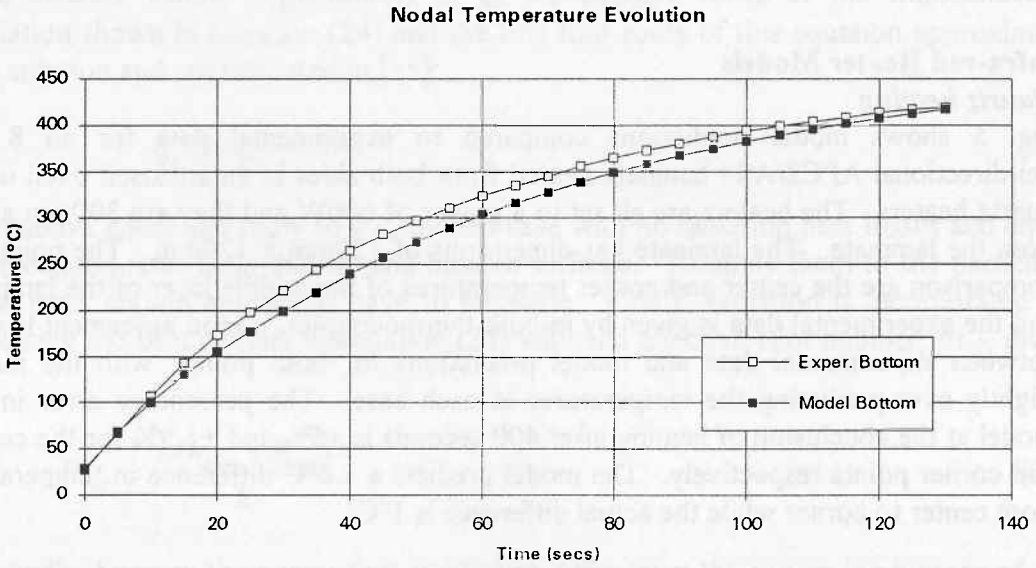

Fig. 6 Comparison of model prediction versus experimental data for a 16 ply APC2/AS4 laminate heated using two sided ceramic heating

Transfer Process Model

Two test cases are shown to validate the transfer process model. The first case is transfer of a laminate after heating by platen radiant heating and the second case is transfer of a laminate after quartz heating.

Case 1 -- Laminate heated using platen radiant heating

The experimental data for this comparison was supplied by Dassault[14]. Fig. 7 shows a comparison between model predictions and experimental data for the center of the top, middle and bottom plies in a 154mm x 1m Cetex panel with 8 plies of varying orientations. The laminate takes 12 secs. to emerge from the oven and another 10 secs. to reach the forming press. If the initial error, where the model under-predicts the heat-up of the laminate, is neglected good agreement occurs between model and experiment. The model predicts correctly that the top node loses the most heat and the middle node loses the least and the curves generally match up well apart from an inaccuracy in the model prediction of the top node temperature after 14 secs. This can possibly be attributed to some convection effect due to the breaking of the vacuum in the platen radiant heating process that is not accounted for in this model.

Case 2 -- Laminate heated using quartz IR heating

In this case a 120mm x 110mm APC2/AS4 uni-directional 16 ply laminate was heated in an infra-red oven using quartz heaters. The laminate was then removed from the oven in 1 sec., transferred over a distance of 2m in 14 secs. and left to stand for 4 secs.

This process simulates a typical transfer process. Fig. 8 compares model predictions to experimental data for three points, all central, one at the top front of the laminate (1), one at the top middle (2) and one just above the bottom ply towards the back of the laminate(3). Once again the model is reasonably accurate. It over-predicts the heat loss slightly for each node. Node 1 loses the most heat, followed by Nodes 2 and 3 and the model predicts this trend also. If the initial inaccuracy of the heat-up calculation is again neglected, then the model predicts Nodes 2 and 3 very well. It is slightly less accurate for Node 1. This can partly be attributed to the fact that this node is at the leading edge of the laminate which is the most difficult part of the laminate to model correctly.

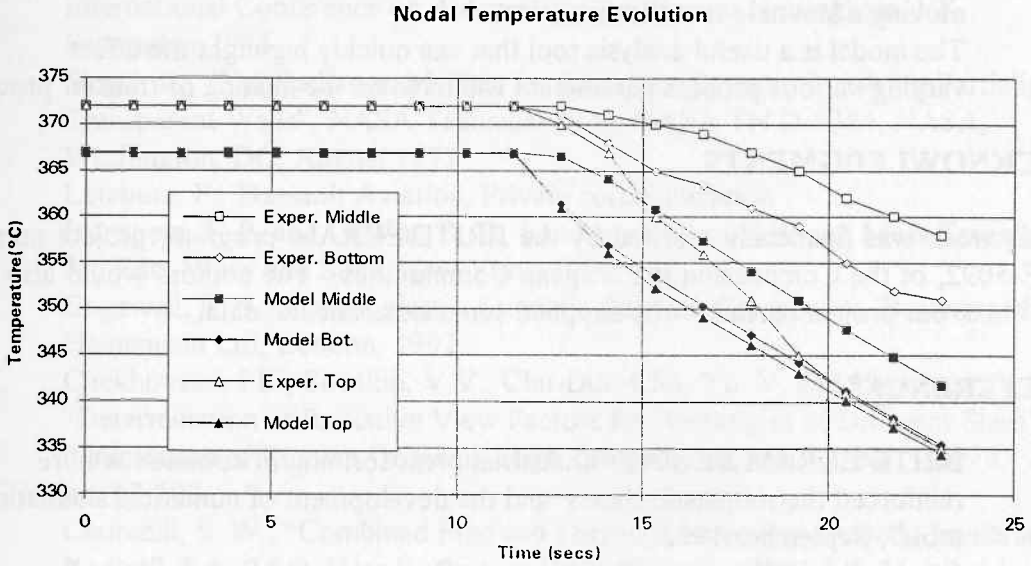

Fig. 7 Comparison of model prediction versus experimental data for an 8 ply Cetex laminate heated using platen radiant heating and then transferred to a forming press

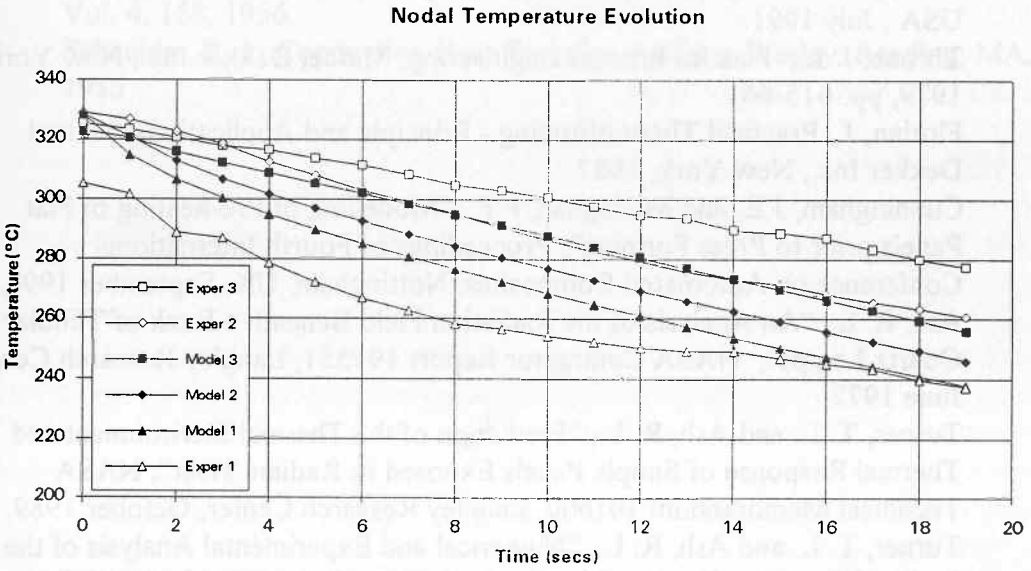

Fig. 8 Comparison of model prediction versus experimental data for a 16 ply APC2/AS4 laminate heated using quartz heating and then transferred out of the heating station

CONCLUSIONS

1. A model has been developed which models the pre-heating of a composite laminate from the start of heating to the point where the forming press first makes contact.
2. The model is general enough to deal with various heating techniques and transfer processes and, despite its generality, it is quite accurate in all cases.
3. The heater models described remove any need for experimentally determined heater temperatures and 'effective emissivities', a simple power input value is all that is needed.
4. The transfer process model gives accurate predictions of the heat lost when moving a laminate to a forming press.
5. The model is a useful analysis tool that can quickly highlight the effect varying various process parameters will have on the heating or transfer process

ACKNOWLEDGMENTS

This work was financially assisted by the BRITE/EURAM program, project number BE-5092, of the Commission if European Communities. The authors would also like to thank our project partners who supplied some experimental data.

REFERENCES

1. BRITE-EURAM BE 5092, "Industrial press forming of continuous fibre reinforced thermoplastic sheets and the development of numerical simulation tools", September 1992.
2. Güçeri, S.L., "Transport Phenomena in Composites Manufacturing - Research Issues and Opportunities", Proceedings of the XXII International Symposium on Manufacturing and Materials Processing, ICHMT, Dubrovnik, August 1990, published by Hemisphere Publishing Corporation, Washington, D.C., USA., July 1991.
3. Throne, J. L., Plastics Process Engineering, Marcel Dekker Inc., New York 1979, pp. 615-661.
4. Florian, J., Practical Thermoforming - Principle and Applications, Marcel Dekker Inc., New York, 1987.
5. Cunningham, J.E. and Monaghan, P.F., "Modelling of Pre-heating of Flat Panels prior to Press Forming", Proceedings of Fourth International Conference on Automated Composites, Nottingham, UK, September 1995.
6. Ash, R. L., "An Analysis of the Radiation Field Beneath a Bank of Tubular Quartz Lamps", NASA Contractor Report 191551, Langley Research Center, June 1972.
7. Turner, T. L. and Ash, R. L., "Prediction of the Thermal Environment and Thermal Response of Simple Panels Exposed to Radiant Heat", NASA Technical Memorandum 101660, Langley Research Center, October 1989.
8. Turner, T. L. and Ash, R. L., "Numerical and Experimental Analysis of the Radiant Heat Flux Produced by Quartz Heating Systems", NASA Technical Paper 3387, Langley Research Center, March 1994.
9. Cassidy, S. F., Monaghan, P. F. and Brogan M. T., "Modelling of infra-red heating of thermoplastic composite panels", Proc. of the 10th Conf. of the Irish

Manufacturing Committee, ed. P. J. Nolan, Vol. 1, University College Galway, Ireland, September 1993.

10. Cassidy, S. F., "Mathematical modelling of infra-red heating of thermoplastic composites in diaphragm forming", Ph.D. thesis, University College Galway, Ireland, 1994.
11. Sweeney, G. J., Monaghan P. F., Brogan M. T., Cassidy S. F., "Reduction of Infra-red (IR) heating cycle time in processing of thermoplastic composites using computer modelling", Composites Manufacturing, Vol. 6(3), September 1995.
12. Brogan, M. T. and Monaghan, P. F., "Thermal Simulation of Quartz Infra-red Heaters used in Processing Thermoplastic Composites", Proc. of the 4th International Conference on Automated Composites, Nottingham, UK, September 1995.
13. Siegel, R., "Net Radiation Method for Enclosure Systems Involving Partially Transparent Walls", NASA Technical Note, NASA TN D-7384, NASA, Washington, DC, August 1973.
14. Lefebure, P., Dassault Aviation, Private communication.
15. Incropera, F. P. and DeWitt, D. P., Fundamentals of Heat and Mass Transfer, 3rd Edn, Wiley and Sons, New York, 1990.
16. Cogswell, F. N., Thermoplastic Aromatic Polymer Composites, Butterworth-Heinemann Ltd, London, 1992.
17. Chekhovskii, I.R., Sirotkin, V.V., Chu-Dun-Chu, Yu. V. and Chebanov, V.A., "Determination of Radiative View Factors for Rectangles of Different Sizes" (Translation of Russian Original), High Temperature, Vol.17, No. 1,1979. pp. 97-100.
18. Churchill, S. W., "Combined Free and Forced Convection Around Immersed Bodies", Sec. 2.5.9, Heat Exchanger Design Handbook, Vol. 2, Hemisphere Publishing, 1983.
19. LeFevre, E. J., "Laminar Free Convection from a Vertical Plane Surface", Proc. of the 9th International Congress on Applied Mechanics, Brussels, Vol. 4, 168, 1956.
20. Schneider, P. J., Conduction Heat Transfer, Addison-Wesley, Reading, MA, 1955.